

Mini Review

Advances in detection of carcinoembryonic antigen for diagnosis of esophageal cancer based on electrochemical aptamer sensors

Haijun Wang^{1,2}, Qiang Guo³, Mingbo Wang¹, Changjiang Liu¹, Ziqiang Tian^{1,*}

¹ Department of Thoracic Surgery, The Fourth Hospital of Hebei Medical University, Shijiazhuang, Hebei 05000, P.R. China

² Department of Thoracic Surgery, Xingtai People's Hospital, Xingtai, Hebei 054000, P.R. China

³ The Affiliated Hospital of Hebei University, Baoding, Hebei, P.R. China

E-mail: ziqiangtian1969@163.com

Received: 23 May 2022 / Accepted: 5 July 2022 / Published: 10 September 2022

The determination of carcinoembryonic antigen (CEA) has been an hot topic in the medical analysis due to the positive correlation between its elevation and many cancers. How to detect CEA with high sensitivity and speed has therefore been of great interest in analytical chemistry. Electrochemical analytical techniques have been considered well suited for screening specific molecules due to their high sensitivity and rapidity. This review summarizes the advances in electrochemical analytical techniques for CEA detection. We divided the electrochemical sensor into impedance, amperage, voltammetry, potentiometry, electrogenerated chemiluminescence (ECL), and photoelectrochemical (PEC). We presented their primary methodologies and important works in them separately. In addition, we compared the performance of recently published sensors through a table. Finally, we present perspectives on this topic based on the review.

Keywords: Electrochemical sensor; Photoelectrochemical sensor; Electrogenated chemiluminescence sensor; Carcinoembryonic antigen; Aptamer

1. INTRODUCTION

According to pathological features, esophageal cancer is classified into esophageal squamous cell carcinoma and esophageal adenocarcinoma. It also includes small cell carcinoma, mucinous epidermoid carcinoma, adenoid cystic carcinoma, and other rare pathological subtypes [1,2]. Esophageal squamous cell carcinoma is a malignant tumor occurring in the mucosal epithelium of the esophagus [3]. Esophageal squamous cell heterogeneous hyperplasia is its precancerous lesion. Patients with mild, moderate, and severe heterogeneous hyperplasia have a progressively higher risk of developing squamous carcinoma with risk factors of 3, 10, and 30 [4], respectively. Esophageal adenocarcinoma is

a malignant tumor that occurs in the esophageal glands. Risk factors include smoking, gastroesophageal reflux, obesity, and genetic susceptibility. The symptoms of early-stage esophageal cancer are not typical, and most patients with esophageal cancer are already in the middle and late stages when they are diagnosed [5–7]. So the 5-year survival rate after surgery is between 15-20%. However, the 5-year survival rate of patients with early-stage esophageal cancer is over 70% after surgery. Therefore, the early diagnosis of esophageal cancer is a hot spot in medical research [8].

Diagnostic methods for esophageal cancer mainly include electronic gastroscopy, ultrasound endoscopy, imaging, and molecular biology markers [9–15]. With the continuous development of molecular biology technology, people began to focus on researching tumor markers related to tumors. It is a group of molecules that reflect the presence of tumors and are rarely found in normal adult tissues [16–19]. Their levels in tumor tissues can be used as an indicator for the presence of a tumor. Tumor markers have been widely applied in clinical practice since the 1960s. Tumor marker testing is easy, economical, and rapid. Some tumor markers are expressed before morphological changes occur in tissues and organs and accompany the whole process of tumor development to the end. Hence, they are of great interest to clinicians. The primary tumor markers used clinically for esophageal cancer detection are carcinoembryonic antigen (CEA), CA19-9, SCC-Ag, and CYFRA21-1 [20–22].

CEA is one of the most widely used tumor-associated antigens among tumor markers. CEA is often highly expressed in colon, breast, and lung adenocarcinomas and most tumors of epithelial origin [23]. It can also be present in the digestive tissues of normal embryos, and trace amounts can be present in normal human serum. It was initially extracted from colonic adenocarcinoma tissue. It was considered a specific tumor marker for colorectal cancer [24–26]. However, it has since been found to be expressed in a variety of tumors, making CEA a broad-spectrum tumor marker [27,28].

Current medical methods for CEA determination are based on immunoassay, including enzyme-linked immunosorbent assay, electrochemical immunoassay, manual radioimmunoassay, immunoradiometric assay, and fluorometric immunoassay [29–33]. While immune-based assays have good selectivity to translate the antigen-antibody binding information into a readable signal. However, these techniques require complex and expensive precision instruments that require specialized technician, and these unfavorable factors limit their widespread use [34–37]. Therefore, the development of rapid, highly sensitive, selective, cost-effective, and efficient CEA assays is of great theoretical significance and application for human disease detection.

Nucleic acid aptamers are single-stranded RNA or DNA molecules selected *in vitro* from a database of nucleic acid molecules obtained by exponentially enriched ligand phylogenetic techniques (SELEX) to specifically bind targets with high affinity [38,39]. It is considered a functional analogue of antibodies. It has a wide range of charge and structural combinations suitable for various biomedical diagnostics, *in vitro* or *in vivo* bioimaging, and therapeutics (Figure 1). Immunosensors have limitations, such as the inability of some tiny molecules to react and the instability of antibodies in extreme environments [40,41] (e.g., high temperatures, harsh acids or bases, etc.). They are therefore not suitable for widespread use in assays [42]. In contrast, nucleic acid aptamers have been widely used in sensor applications because of their high flexibility, reproducibility, ease of immobilization, lack of batch-to-batch variation, and reproducibility [43].

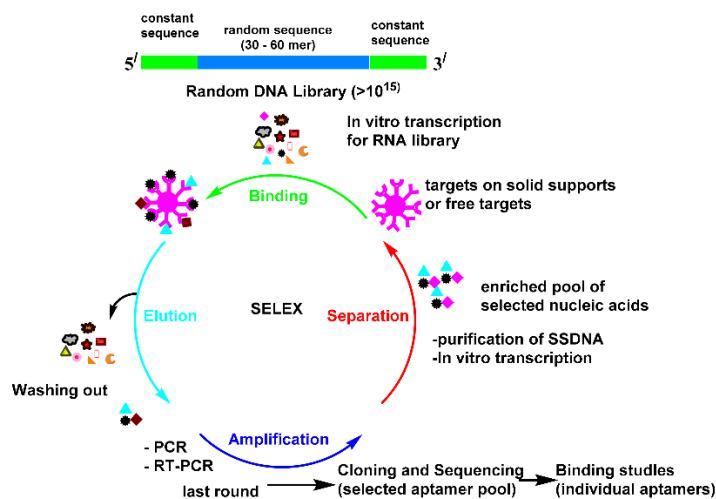


Figure 1. Systematic development of ligands by SELEX (reused under Creative Commons license, MDPI) [44].

Electrochemical biosensors are based on a selective interaction between the target molecules and the recognition element to produce an electrical signal proportional to the molecule concentration [45,46]. A typical electrochemical biosensor consists of the working electrode, reference electrode, and counter electrode. Various electrochemical techniques are now used in CEA sensing applications, including impedance, amperage, voltammetry, potentiometry, electrogenerated chemiluminescence (ECL), and photoelectrochemical (PEC) [47,48]. This review summarizes the electrochemical detection of CEA through these five different types of aptamer sensors. We present information about these sensors and representative work on them. Finally, we also present perspectives on the development of this topic.

Detection of CEA via EIS based aptamer sensor

EIS biosensors measure changes in the electrical impedance spectrum resulting from the interaction between analyte and electrode. The EIS biosensor platform is informative, non-destructive, simple, and label-free and has received much attention from researchers.

Zhou et al. [49] reported an electrochemical impedance nucleic acid aptamer sensor for CEA determination. The functionalized copper-based metal-organic (Pt@CuMOFs-hGq-GOx) was constructed via the glucose oxidase (GOx)-driven cascade catalytic amplification. The Pt@CuMOFs and hemin/G-quadruplexes (hGq) catalyze the H₂O₂ reduction via the cascade reaction. In another work, the electrochemical impedance signal was significantly enhanced by the oxidation of 3,3-diaminobenzidine and the formation of insoluble precipitates, which are non-conductive. It has a LOD of 0.023 pg/mL with a linear range of 0.05 pg/mL to 20 ng/mL. In addition, they constructed a sensitive biosensing interface for CEA analysis [50]. CEA and its aptamer were used as a test model for the impedance-based aptasensor proposed in this paper. Nanocarriers made of PtPd nanowires with a huge surface area and high conductivity were used to load biomolecules substantially. Then, with the help of a DNA initiator, two DNA hairpins were inserted to initiate HCR, resulting in the development of a lengthy dsDNA

scaffold. In the same time, MnTMPyP molecules, which imitate the enzyme MnTMP, were implanted into the resulting dsDNA in situ, resulting in the complex MnTMPyP-dsDNA with peroxidase-like activity. 3,3-diaminobenzidine was oxidized to create non-conductive insoluble precipitates under biocatalysis. Consequently, electron transmission was greatly hampered, resulting in considerable electrochemical impedimetric signal amplification. As a result, the suggested aptasensor's analytical performance was considerably enhanced, with a LOD of 0.030 pg/mL. Yen et al. [51] developed a EIS aptasensor using graphene and PEDOT:PSS-modified paper (Figure 2).

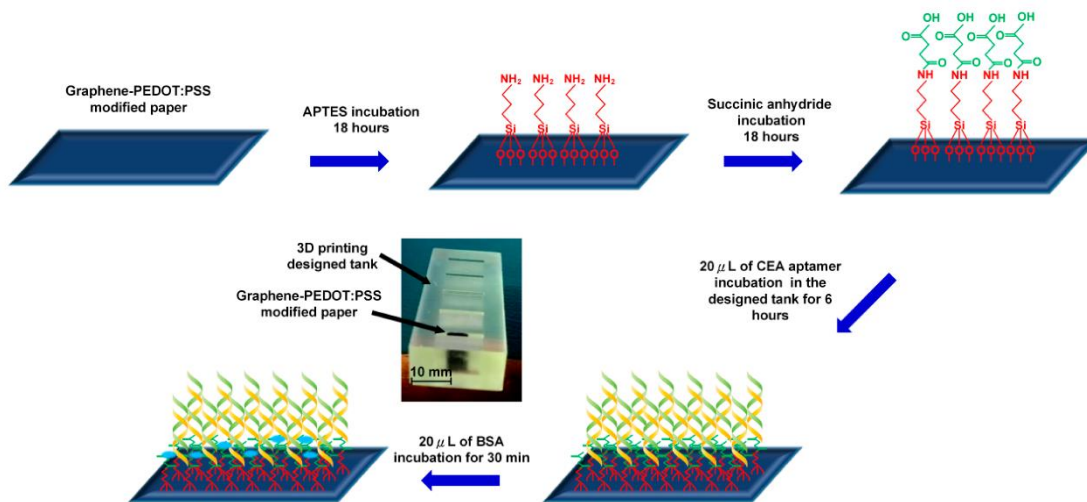


Figure 2. Schematic diagram of fabrication of graphene/PEDOT:PSS based EIS aptamer sensor (reused under Creative Commons license, MDPI) [51].

Table 1. Recent published EIS aptamer sensor for CEA detection and their performance.

Signal amplification method	Linear detection range	LOD	Reference
Pt@CuMOFs-hGq-GOx	0.05 pg/mL-20 ng/mL	0.023 pg/mL	[49]
PtPdNWs, MnTMPyP, and HCR	0.1 pg/mL-40 ng/mL	0.030 pg/mL	[50]
Graphene/PEDOT:PSS	0.77–14 ng/mL	0.45 ng/mL	[51]
M/CEA-A/Au/SPE	0.2–15.0 ng/mL	0.085 ng/mL	[52]
AgNC@Apt@UiO-66	0.01–10 ng/mL	0.3 ng/mL	[53]
AuNPs-amino-functionalized MCM-41/GCE	0.001-100.0 ng/mL	0.00098 ng/mL	[54]
NiCoPBA-based aptasensor	1.0 fg/mL-5.0 ng/mL	0.74 fg/mL	[55]

The nanocomposite provides a conductive and sensitive substrate for further aptamer functionalization. This inexpensive paper-based aptasensor detects CEA in human blood samples and

reference buffer solutions across a linear range of 0.77–14 ng/L. The LOD of CEA in both sample is 0.45 ng/mL and 1.06 ng/mL, respectively. The evaluation of this aptamer-based sensing device revealed a strong connection with the immunoassay detection approach. The suggested aptasensor has proved its promise as a quick, simple point-of-care (POC) sensor for early cancer detection in regions with limited manufacturing capabilities, analytical equipment, and trained experts. Table 1 summarizes the current published EIS aptamer sensor for CEA detection.

Detection of CEA via amperometric based aptamer sensor

Amperometric biosensors measure the increase of the current generated by a constant reduction or oxidation potential applied to the working electrode. Amperometric biosensors measure current as a function of independent variables, such as time or electrode potential. Therefore, current-based biosensors are well suited for detecting electroactive molecules.

Shu et al. [56] reported a novel electrochemical nucleic acid aptamer sensor based on signal amplification of AuNPs. Compared to a single nucleic acid aptamer, they used two different nucleic acid aptamers for CEA detection. This method yielded an advance accuracy with a low background signal and excellent selectivity. Wang et al. [57] fabricated an electrochemical sensor based on a template-independent enzymatic polymerization reaction initiated by a nucleic acid aptamer. Nucleic acid aptamer 1 attached to the Au electrode for capturing probe, and nucleic acid aptamer 2 modified on the AuNPs surface is used as a nanoprobe. The capture probe and nanoprobe form a sandwich structure with the CEA. After that, efficient amplification by terminal deoxynucleotidyl transferase and anti-biotin protein-modified horseradish peroxidase significantly enhanced the sensing performance.

Paniagua et al. [58] reported the invention of a biosensing technique for the recognition of CEA using Janus NPs as an integrated electrochemical recognition system. It had horseradish peroxidase on the surface of the Janus nanoparticles so that they could be used as a signaling element. The sensing strategy depends on the particular initial identification of CEA by the bifunctionalized Janus nanoparticles, which causes the DNA hairpin structure to expand and reveals the biotin residues in the aptamer chain. This CEA-Janus nanoparticle combination was then collected, enabling further magnetic deposition on SPE for amperometric determination of the CEA. Table 2 summarizes the current published amperometric aptamer sensor for CEA detection.

Table 2. Recent published amperometric aptamer sensor for CEA detection and their performance.

Signal amplification method	Linear detection range	LOD	Reference
Apt2–AuNPs–Fc	1 to 200 ng/mL	0.5 ng/mL	[56]
Aptamer-OTEP	5 fM–500 nM	5 fM	[57]
SPCE/NanoCaptors/JNP3	1–5000 ng/mL	210 pg/mL	[58]
GCE/Gr-DN-AuNPs/Ab1	0.01–120 ng/mL	8 pg/mL	[59]
Apt/AuNP/rGO/SPE	20 pg/mL–2 µg/mL	16 pg/mL	[60]

Detection of CEA via potentiometric based aptamer sensor

Potentiometric biosensors measure the potential difference between the working electrode and the reference electrode caused by a change in the concentration of a charged substance. Field-effect transistors (FETs) are a particular type of potentiometric biosensor. The combination of charged substance causes a change in the intrinsic carrier concentration in the FET channel, which allows the FET to be recognized by the bioassay. This sensor is label-free and has high sensitivity, selectivity, and repeatability.

Park et al. [61] applied nucleic acid aptamer-functionalized multidimensional conducting polymer (3-carboxylate polypyrrole) nanotubes (Apt-C-PPy MNT) to prepare FET biosensor for CEA determination (**Figure 3**). A temperature-controlled method for the solution synthesizes the multidimensional system C-PPy MNT and immobilizes it on the electrode surface. It is then binding with the amine-modified CEA nucleic acid aptamer via amide bonding. The C-PPy MNT-based FET sensor has a fast response (< -1s) and good conductivity for CEA determination. The response intensity increases with increasing CEA concentration, with approximately 1 fg/mL detection limit. Chen et al. [62] demonstrated using phenylboronic acid-functionalized CaCO₃ NPs in conjunction with a portable Ca²⁺ ion-selective electrode to detect the CEA. CaCO₃ NPs were coupled to 3-aminophenylboronic acid, whereas the target CEA was trapped at the aptasensory interface. Based on the sugar-boronic acid interaction, 3-aminophenylboronic acid is selectively recognized by the CEA to form a complex. CaCO₃ was dissolved in acidic circumstances to liberate Ca²⁺ ions, as measured using a portable ion-selective electrode. Under optimal circumstances, the aptasensing platform displayed a strong electrode potential response for assessing target CEA and permitted the determination of CEA at concentrations of 7.3 pg/mL. Hong et al. [63] established a potentiometric aptasensor for the determination of CEA in human blood using a graphene oxide (GO) modified GCE through target recycling-assisted signal amplification. Initially, the GO were fixed on the electrode by physical adsorption. The GO was then coated with CEA aptamers through stacking interaction. Upon introducing the target CEA, the analyte interacted with the aptamer to create a complex, leading to the aptamer's separation. In the presence of DNase I, the generated CEA–aptamer complexes were cleaved to liberate target CEA, therefore initiating target catalysis. Dissociation of aptamers from GO may alter the local electrical potential. Under optimal circumstances, the potential shift increased with CEA concentrations and displayed strong potential responses throughout a linear range of 0.01–100 ng/mL with a LOD of 9.4 pg/mL. The accuracy of this sensor was assessed for the examination of human blood, yielding findings that corresponded well with those from a commercially available human CEA ELISA kit. Comparatively, the potentiometric aptamer sensor was rarely used in CEA. This may be due to the limited detection range of potentiometric sensing.

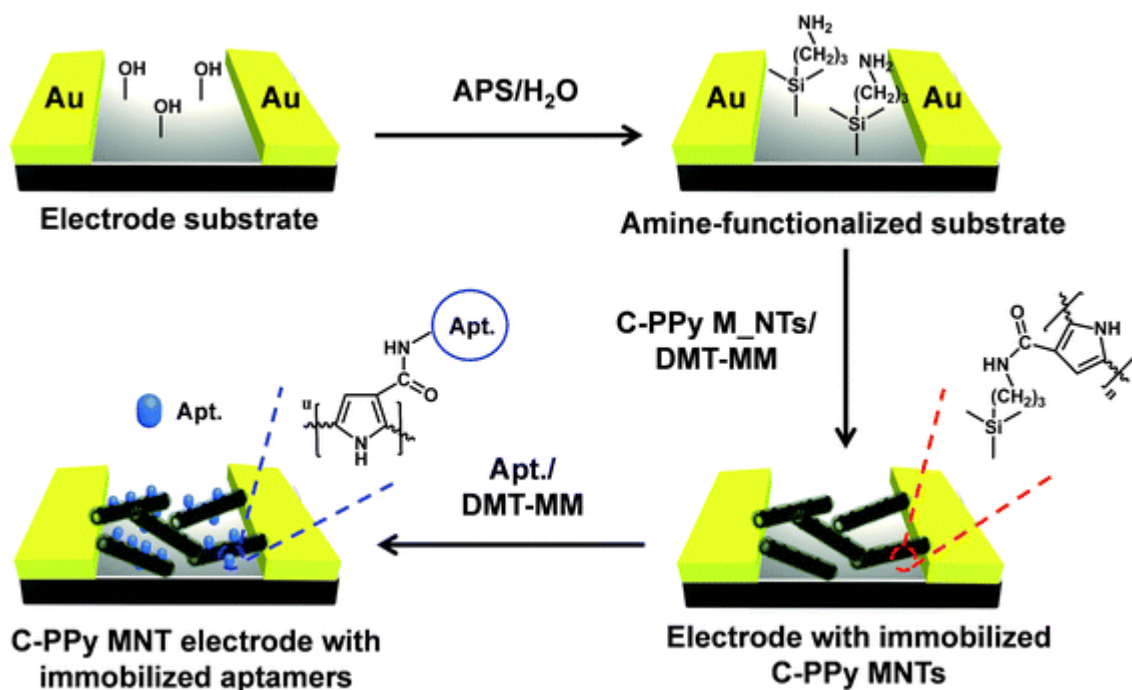


Figure 3. Schematic diagram of a FET based potentiometric biosensor (reused under Creative Commons license, RSC) [61].

Detection of CEA via voltammetric based aptamer sensor

The techniques used for voltammetric aptamer sensors include cyclic voltammetry (CV), square wave voltammetry (SWV), and differential pulse voltammetry (DPV). They allow simple, sensitive, highly specific, and strongly applicable determination of low-level protein. Voltammetric biosensors allow low correlation noise to be observed, thus providing reliable and reproducible signal for analyte quantification. Moreover, voltammetry can detect multiple analytes in a single electrochemical experiment, thus allowing the simultaneous detection.

Huang et al. [100] fabricated an aptamer sensor via the Pb²⁺-dependent DNA enzyme-assisted signal amplification and graphene quantum dot ionic liquid-ion (GQDs-IL-NF) composite membrane for CEA sensing. Hairpin DNA containing a CEA aptamer and a DNAzyme chain can identify the analyte and forms a complex in the presence of CEA. The DNAzyme-assisted signal amplification reaction can produce ssDNA. π - π stacking can adsorb ssDNA onto GCE with methylene blue-labeled DNA and produces an electrochemical signal. The sensor exhibited a linear range of 0.5 fg/mL to 0.5 ng/mL with a LOD of 0.34 fg/mL. Another electrochemical aptasensor for CEA sensing based on polydopamine functional graphene and Pd-Pt nanodendrites was reported by Zhang et al. [64]. The hemin/G-quadruplex (hemin/G4) conjugation has peroxidase-like activity. First, the electrode surface was coated with polydopamine functional graphene to fix CEA aptamer 1. The secondary aptamer was then made using polydopamine functional graphene and Pd-Pt nanodendrites for immobilizing hemin/G4. The second aptamer was caught on the sensing surface as a result of the sandwich-type specific interaction between CEA and the matching aptamers. It may increase current signals by catalyzing the oxidation of signal probe with H₂O₂. In addition, the electrochemical signals of

hydroquinone were proportional to the concentrations of CEA. Furthermore, the suggested technique has acceptable sensitivity and stability and high accuracy in real-world applications.

The hollow N-doped carbon nanoboxes (N-C n-box) have garnered a great deal of interest owing to their exceptional characteristics and their substantial intrinsic cavities that are appropriate for immobilizing certain compounds. Rahmati et al. [65] developed a N-C n-box based aptasensor that uses thionine (Thi) as the signal molecule. CEA was measured using aptamer strings immobilized on AuNPs and N-C N-boxes, employed as signal amplifiers and substrates. The target molecule obstructs electron transport, resulting in a reduction in Thi-associated SWV peak currents. This method lowers the distance between the redox probe and the electrode surface while increasing the quantity of redox probes. This approach demonstrated greater sensitivity and broader linearity in 0.1 fM to 30 nM. Table 3 summarizes the recently published voltammetric aptamer sensor for CEA detection.

Table 3. Recent published voltammetric aptamer sensor for CEA detection and their performance.

Signal amplification method	Linear detection range	LOD	Reference
MB-substrate/GQDs-IL-NF/GCE	0.5 fg/mL-0.5 ng/mL	0.34 fg/mL	[66]
TDN and CHA	1–30000 pg/mL	0.04567 pg/mL	[67]
Pd-PtNDs/PDA@Gr	0.050–1000 ng/mL	6.3 pg/mL	[64]
ConA/HRP	5.0–40 ng/mL	3.4 ng/mL	[68]
NCMTs@Fe ₃ O ₄ @Cusilicate	0.030–6.0 ng/mL	5.4 pg/mL	[69]
Thi@N-C n-box/AuNPs	17 fg/mL–5.4 ng/mL	5 fg/mL	[65]
Hybrid DNA /CEA-H1/BSA/MCH/H2/Au	10 pg/mL–100 ng/mL	0.84 pg/mL	[70]
Hemin/H1-H2/DMP/MCH/DTPs/Au	0.0001–50 ng/mL	0.0182 pg/mL	[71]
CNTs-PFcGE	1 fg/mL-10 ng/mL	0.28 fg/mL	[72]
HGNs-MWCNTs	1 fg/mL-10 ng/mL	0.82 fg/mL	[73]
HGNs-AuNPs	0.1 pg/mL-10 ng/mL	40 fg/mL	[74]

Detection of CEA via ECL based aptamer sensor

ECL is light produced by electron transfer reactions between electrochemically generated reagents. ECL combines electrochemical controllability with a low chemiluminescence background, offering the advantages of low cost, simple optical setup, and fast measurements.

Wang et al. [75] designed a biosensor based on Ru(bpy)₃²⁺ surface-enhanced ECL for ultrasensitive detection of CEA. Ru(bpy)₃²⁺-doped SiO₂ NPs were applied as ECL emitters. AuNPs were used as a localized surface plasmon resonance source to enhance the ECL signal. In the presence of

CEA, Ru(bpy)₃²⁺-doped SiO₂ NPs and AuNPs form a nanostructured network that increases the ECL intensity by a factor of 30. The biosensor has a LOD of 1.52 fg/mL with a linear range of 5 fg/mL to 50 pg/mL. In another work, Wang et al. [76] used ZnS-CdS NPs-MoS₂ modified electrode as a detection platform for CEA sensing. The MoS₂ on the electrode extends the surface area, which significantly increases the ZnS/CdS immobilization and produces an enhanced ECL signal with a LOD of 0.031 ng/mL. Wei et al. [77] proposed an ECL sensor based on CdS QDs loaded on MOF for sensitive assessment of CEA. Due to the weak conductivity of CEA, the ECL signals were reduced after incubation in CEA solution, and there was association between ECL intensity and the concentration of CEA. The LOD can be calculated to be 0.085 pg/mL. The sensing performance of the proposed ECL aptasensor for detecting CEA in human blood was excellent. Shi et al. [78] reported an ECL aptasensor for CEA sensing based on the ECL of CdS-graphene with peroxydisulfate as the co-reactant. CdS-GR were produced using a simple one-pot solvothermal technique and then immobilized on the GCE surface. L-Cystine (L-cys) can significantly boost electron transport and ECL intensity. AuNPs were constructed for aptamer immobilization and ECL signal amplification. Through an Au-S link, the thiol-modified aptamer was adsorbed on the AuNPs. The LOD of the ECL sensor is 3.8 pg/mL, while the ECL intensity is linear with the CEA concentration in 0.01–10.0 ng/mL. The constructed aptasensor was used to measure CEA levels in human serum samples. The CEA recoveries in human serum samples ranged from 85.0% to 109.5%, and the RSD values did not exceed 3.4%. Table 4 summarizes the recently published ECL aptamer sensor for CEA determination.

Table 4. Recent published ECL aptamer sensor for CEA detection and their performance.

Signal amplification method	Linear detection range	LOD	Reference
Ru@SiO ₂ -AuNPs	5 fg/mL-50 pg/mL	1.52 fg/mL	[75]
ZnS-CdS/MoS ₂ /GCE	0.05-20 ng/mL	0.031 ng/mL	[76]
CEA/β-ME/Apt/TEOA@Au/CdS QDs@MOF/GCE	0.0004-10 ng/mL	0.085 pg/mL	[77]
BSA/aptamer/AuNPs/L-cys/Nafion/CdS-GR/GCE	0.01–10.0 ng/mL	3.8 pg/mL	[78]
QD probe DNA/Au NPs/electrode	1.0 fg/mL-100 ng/mL	0.21 fg/mL	[79]
GCE/Au/dsDNA/MCH/CEA/Cu NCs	0.2 fg/mL-1 ng/mL	66.67 ag/mL	[80]
BCP/H-rGO-aptamer II/CEA/BSA/NH ₂ -DNA/Au-CdS-CS/GCE	0.8 pg/mL-4 ng/mL	0.28 pg/mL	[81]
Double-check mode based ECL aptasensor using Ag-PAMAM NCs	0.001–500 ng/mL	0.39 pg/mL	[82]
luminol-hemin@MIL-88B (Fe)-H ₂ O ₂ -N ₂	0.01–100 ng/mL	1.5 pg/mL	[83]

Detection of CEA via PEC based aptamer sensor

PEC biosensors combine the advantages of efficient sensing techniques of electrochemistry and photochemistry with a lower background signal and are more sensitive than conventional electrochemical methods. At the same time, it does not require the complex and expensive instrumentation cost and has attracted increasing attention.

Ge et al. [84] fabricated a PEC sensor that uses catalytic hairpin assembly (CHA) and hybridization chain reaction for cascade secondary signal amplification to detect CEA. In the presence of CEA, single-stranded trigger-DNA is released from the CEA-apt@sstDNA complex, triggering upstream CHA recirculation. The dsDNA complex generated by CHA further induces downstream HCR amplification, leading to numerous hemin/G-quadruplex DNases. This can produce the insoluble/insulating product formed by the biocatalytic precipitation of 4-chloro-1-naphthol, resulting in a significant reduction of the photocurrent signal. Qiu et al. [85] presented a novel PEC aptasensor powered by NIR light for sensitive screening of CEA. The upconversion nanoparticles (UCNs) potentially transform NIR light into a wavelength that semiconductors can collect. Effectively amplifying the photocurrent, the produced Ag₂S may exploit the upconversion emissions. For the analysis of target CEA, this approach could achieve excellent accuracy and specificity. Using our method, human blood samples containing target CEA were evaluated, and the findings were well-matched to human CEA enzyme-linked immunosorbent test kits. Table 5 summarizes the current published PEC aptamer sensor for CEA detection.

Table 5. Recent published PEC aptamer sensor for CEA detection and their performance.

Signal amplification method	Linear detection range	LOD	Reference
CHA-based single-recycling amplification strategy	8.0 fg/mL-50.0 pg/mL	8.0 fg/mL	[84]
NaYF ₄ :Yb,Er	0.005–5.0 ng/mL	1.9 pg/mL	[85]
Core-shell	-	3.6 pg/mL	[86]
NaYF ₄ :Yb,Tm@TiO ₂	-	0.032 ng/mL	[87]
NaYF ₄ :Yb,Tm@ZnO	-	0.032 ng/mL	[87]
NaYF ₄ :Yb,Er	10.0 pg/mL–5.0 ng mL	4.8 pg/mL	[88]
UCNPs@CdTe	-	-	-
Au/BiVO ₄ /CdS QDs	0.0001–10 ng/mL	0.047 pg/mL	[89]
g-C ₃ N ₄ /CuInS ₂ and CoOOH	0.02–40 ng/mL	5.2 pg/mL	[90]
CdTe QDs/RGO-AuNPs	0.001 to 2.0 ng/mL	0.47 pg/mL	[91]
D-A F8BT/g-C ₃ N ₄ /AuNPs	0.02-50 ng/mL	6.7 pg/mL	[92]
TiO ₂ @Au NPs/CdS QDs	-	18.9 fg/mL	[93]
ZnO flower-rod/g-C ₃ N ₄ -Au	0.01 ng/mL-2.5 ng/mL	1.9 pg/mL	[94]
Au@CuS-GR	0.1 pg/mL-10 ng/mL	59.9 fg/mL	[95]

2. CONCLUSION

CEA detection has long been an important topic in electrochemical analysis because it has a significant role in clinical diagnosis. Aptamer-based electrochemical analysis for CEA detection can be divided into five different types. Voltammetry-based and PEC-based aptamer electrochemical biosensors are the two most investigated types. This is due to their complex methodological constructs that can achieve CEA's highly sensitive and specific identification. In contrast, potentiometric and current-based sensors are difficult to achieve highly sensitive linear detection due to the small variability of the detected signals. Although biosensors based on electrochemical aptamer technology have been able to achieve sensitive detection of CEA, even up to aM level in some work, they face some challenges in being used in practice for detection. Today, ECL and PEC sensors are only available for laboratory testing and not for POC detection, so they are not particularly superior to conventional analytical means. Other sensors can be miniaturized, but the detection steps are still cumbersome and subject to environmental influences.

ACKNOWLEDGEMENT

Authors acknowledged the financial support of specific project of the national cancer center of China on the scientific research of oncology (No. NCC2017A24; The correlations between the expression of long noncoding RNA (SPRY4-IT1) and the lymph node metastasis in esophageal squamous cell carcinoma).

References

1. L. Zhao, M. Cheng, G. Liu, H. Lu, Y. Gao, X. Yan, F. Liu, P. Sun, G. Lu, *Sens. Actuators B Chem.*, 273 (2018) 185–190.
2. Z. Wang, X. Tian, D. Sun, P. Cao, M. Ding, Y. Li, N. Guo, R. Ouyang, Y. Miao, *RSC Adv.*, 10 (2020) 15870–15880.
3. N. Gan, L. Jia, L. Zheng, *Int. J. Mol. Sci.*, 12 (2011) 7410–7423.
4. A. Jing, Q. Xu, W. Feng, G. Liang, *Micromachines*, 11 (2020) 660.
5. J. Wu, Z. Fu, F. Yan, H. Ju, *TrAC Trends Anal. Chem.*, 26 (2007) 679–688.
6. X. Xiao, X. Zhang, G. Qin, *J. Mod. Lab. Med.* (2017) 72–75.
7. Y. Chen, J.-J. Feng, L.-P. Mei, C.-G. Shi, A.-J. Wang, *J. Colloid Interface Sci.*, 555 (2019) 647–654.
8. D. Sadighbayan, K. Sadighbayan, M.R. Tohid-Kia, A.Y. Khosroushahi, M. Hasanzadeh, *TrAC Trends Anal. Chem.*, 118 (2019) 73–88.
9. L.-Y. Sun, Z.-M. Du, Y.-Y. Liu, Y.-H. Li, X.-M. Liu, T. Wang, J.-Y. Shao, *Cancers*, 13 (2021) 664.
10. X.-Y. Chu, X.-B. Hou, W.-A. Song, Z.-Q. Xue, B. Wang, L.-B. Zhang, *Cancer Biol. Ther.*, 11 (2011) 995–1000.
11. M. Hasanzadeh, N. Shadjou, M. de la Guardia, *TrAC Trends Anal. Chem.*, 91 (2017) 67–76.
12. J. Zhuang, H. Wan, X. Zhang, *Talanta*, 225 (2021) 121981.
13. H. Karimi-Maleh, Y. Orooji, F. Karimi, M. Alizadeh, M. Baghayeri, J. Rouhi, S. Tajik, H. Beitollahi, S. Agarwal, V.K. Gupta, *Biosens. Bioelectron.* (2021) 113252.
14. H. Karimi-Maleh, A. Khataee, F. Karimi, M. Baghayeri, L. Fu, J. Rouhi, C. Karaman, O. Karaman, R. Boukherroub, *Chemosphere* (2021) 132928.
15. H. Karimi-Maleh, F. Karimi, L. Fu, A.L. Sanati, M. Alizadeh, C. Karaman, Y. Orooji, *J. Hazard. Mater.*, 423 (2022) 127058.
16. Y. Yue, L. Su, M. Hao, W. Li, L. Zeng, S. Yan, *Front. Chem.*, 9 (2021) 479.

17. S. Yan, Y. Yue, L. Zeng, L. Su, M. Hao, W. Zhang, X. Wang, *Front. Chem.*, 9 (2021) 220.
18. T.A. Tabish, H. Hayat, A. Abbas, R.J. Narayan, *Curr. Opin. Electrochem.*, 30 (2021) 100786.
19. N.J. Ronkainen, S.L. Okon, *Materials*, 7 (2014) 4669–4709.
20. R. Eivazzadeh-Keihan, P. Pashazadeh-Panahi, B. Baradaran, A. Maleki, M. Hejazi, A. Mokhtarzadeh, M. de la Guardia, *TrAC Trends Anal. Chem.*, 100 (2018) 103–115.
21. D. Sadighbayan, K. Sadighbayan, A.Y. Khosroushahi, M. Hasanzadeh, *TrAC Trends Anal. Chem.*, 119 (2019) 115609.
22. H. Karimi-Maleh, M. Alizadeh, Y. Orooji, F. Karimi, M. Baghayeri, J. Rouhi, S. Tajik, H. Beitollahi, S. Agarwal, V.K. Gupta, S. Rajendran, S. Rostamnia, L. Fu, F. Saberi-Movahed, S. Malekmohammadi, *Ind. Eng. Chem. Res.*, 60 (2021) 816–823.
23. E.C. Rama, A. Costa-García, *Electroanalysis*, 28 (2016) 1700–1715.
24. L. Shang, X. Wang, W. Zhang, L.-P. Jia, R.-N. Ma, W.-L. Jia, H.-S. Wang, *Sens. Actuators B Chem.*, 325 (2020) 128776.
25. T. Špringer, J. Homola, *Anal. Bioanal. Chem.*, 404 (2012) 2869–2875.
26. W. Ye, Y. Zheng, P. Zhang, B. Fan, Y. Li, L. Fu, *Int J Electrochem Sci*, 16 (2021) 211041.
27. Y. Yu, Q. Zhang, J. Buscaglia, C.-C. Chang, Y. Liu, Z. Yang, Y. Guo, Y. Wang, K. Levon, M. Rafailovich, *Analyst*, 141 (2016) 4424–4431.
28. S.H. Shamsuddin, T.D. Gibson, D.C. Tomlinson, M.J. McPherson, D.G. Jayne, P.A. Millner, *Biosens. Bioelectron.*, 178 (2021) 113013.
29. L.P. Carneiro, N.S. Ferreira, A.P. Tavares, A.M. Pinto, A. Mendes, M.G.F. Sales, *Biosens. Bioelectron.*, 175 (2021) 112877.
30. M. Wu, C. Zhao, Y. Yang, K. Cao, X. Qiao, C. Hong, *Electroanalysis*, 32 (2020) 1329–1336.
31. M. Rizwan, S. Elma, S.A. Lim, M.U. Ahmed, *Biosens. Bioelectron.*, 107 (2018) 211–217.
32. H. Karimi-Maleh, C. Karaman, O. Karaman, F. Karimi, Y. Vasseghian, L. Fu, M. Baghayeri, J. Rouhi, P. Senthil Kumar, P.-L. Show, S. Rajendran, A.L. Sanati, A. Mirabi, *J. Nanostructure Chem.* (2022).
33. H. Karimi-Maleh, H. Beitollahi, P.S. Kumar, S. Tajik, P.M. Jahani, F. Karimi, C. Karaman, Y. Vasseghian, M. Baghayeri, J. Rouhi, *Food Chem. Toxicol.* (2022) 112961.
34. C. Wang, Y. Wang, H. Zhang, H. Deng, X. Xiong, C. Li, W. Li, *Anal. Chim. Acta*, 1090 (2019) 64–71.
35. L. Huang, Z. Yu, J. Chen, D. Tang, *ACS Appl. Bio Mater.*, 3 (2020) 9156–9163.
36. H. Karimi-Maleh, A. Ayati, S. Ghanbari, Y. Orooji, B. Tanhaei, F. Karimi, M. Alizadeh, J. Rouhi, L. Fu, M. Sillanpää, *J. Mol. Liq.*, 329 (2021) 115062.
37. H. Karimi-Maleh, A. Ayati, R. Davoodi, B. Tanhaei, F. Karimi, S. Malekmohammadi, Y. Orooji, L. Fu, M. Sillanpää, *J. Clean. Prod.*, 291 (2021) 125880.
38. Y. Bai, H. Zhang, L. Zhao, Y. Wang, X. Chen, H. Zhai, M. Tian, R. Zhao, T. Wang, H. Xu, *Talanta*, 221 (2021) 121451.
39. S.M. Taghdisi, N.M. Danesh, M. Ramezani, A.S. Emrani, K. Abnous, *Electroanalysis*, 30 (2018) 1734–1739.
40. M.I.A. de Melo, C.R. Correa, P. da Silva Cunha, A.M. de Góes, D.A. Gomes, A.S.R. de Andrade, *Bioorg. Med. Chem. Lett.*, 30 (2020) 127278.
41. Q.-L. Wang, H.-F. Cui, J.-F. Du, Q.-Y. Lv, X. Song, *RSC Adv.*, 9 (2019) 6328–6334.
42. S. Lisi, E. Fiore, S. Scarano, E. Pascale, Y. Boehman, F. Ducongé, S. Chierici, M. Minunni, E. Peyrin, C. Ravelet, *Anal. Chim. Acta*, 1038 (2018) 173–181.
43. X. Lin, S. Li, B. Zhang, H. Yang, K. Zhang, H. Huang, *Anal. Methods*, 12 (2020) 5496–5502.
44. A.-E. Radi, M.R. Abd-Ellatief, *Diagnostics*, 11 (2021) 104.
45. Q.-L. Wang, H.-F. Cui, C.-L. Li, X. Song, Q.-Y. Lv, Z.-Y. Li, *Sens. Actuators Rep.*, 2 (2020) 100021.
46. Q. Shu, Y. Zhu, Y. Xiao, K. Chen, X. Mai, X. Zheng, X. Yan, *Microchem. J.* (2022) 107482.
47. A. Villalonga, A.M. Pérez-Calabuig, R. Villalonga, *Anal. Bioanal. Chem.*, 412 (2020) 55–72.

48. R. Lu, S. Li, M. Fan, J. Wei, X. Liu, *RSC Adv.*, 8 (2018) 14663–14668.
49. X. Zhou, S. Guo, J. Gao, J. Zhao, S. Xue, W. Xu, *Biosens. Bioelectron.*, 98 (2017) 83–90.
50. X. Zhou, S. Xue, P. Jing, W. Xu, *Biosens. Bioelectron.*, 86 (2016) 656–663.
51. Y.-K. Yen, C.-H. Chao, Y.-S. Yeh, *Sensors*, 20 (2020) 1372.
52. Y. Wang, L. Chen, T. Xuan, J. Wang, X. Wang, *Front. Chem.* (2021) 569.
53. C. Guo, F. Su, Y. Song, B. Hu, M. Wang, L. He, D. Peng, Z. Zhang, *ACS Appl. Mater. Interfaces*, 9 (2017) 41188–41199.
54. Z. Shekari, H.R. Zare, A. Falahati, *J. Electrochem. Soc.*, 164 (2017) B739–B745.
55. L. He, Z. Li, C. Guo, B. Hu, M. Wang, Z. Zhang, M. Du, *Sens. Actuators B Chem.*, 298 (2019) 126852.
56. H. Shu, W. Wen, H. Xiong, X. Zhang, S. Wang, *Electrochem. Commun.*, 37 (2013) 15–19.
57. P. Wang, Y. Wan, S. Deng, S. Yang, Y. Su, C. Fan, A. Aldalbahi, X. Zuo, *Biosens. Bioelectron.*, 86 (2016) 536–541.
58. G. Paniagua, A. Villalonga, M. Eguílaz, B. Vegas, C. Parrado, G. Rivas, P. Díez, R. Villalonga, *Anal. Chim. Acta*, 1061 (2019) 84–91.
59. J. Huang, J. Tian, Y. Zhao, S. Zhao, *Sens. Actuators B Chem.*, 206 (2015) 570–576.
60. A. Villalonga, B. Vegas, G. Paniagua, M. Eguílaz, B. Mayol, C. Parrado, G. Rivas, P. Díez, R. Villalonga, *J. Electroanal. Chem.*, 877 (2020) 114511.
61. J.W. Park, W. Na, J. Jang, *RSC Adv.*, 6 (2016) 14335–14343.
62. Y. Chen, B. Li, P. Lyu, H.F. Kwok, L. Ge, Q. Wu, *Anal. Bioanal. Chem.*, 413 (2021) 1073–1080.
63. Z. Hong, G. Chen, S. Yu, R. Huang, C. Fan, *Anal. Methods*, 10 (2018) 5364–5371.
64. F. Zhang, Z. Liu, Y. Han, L. Fan, Y. Guo, *Bioelectrochemistry*, 142 (2021) 107947.
65. Z. Rahmati, M. Roushani, H. Hosseini, *J. Electroanal. Chem.*, 903 (2021) 115858.
66. J.-Y. Huang, L. Zhao, W. Lei, W. Wen, Y.-J. Wang, T. Bao, H.-Y. Xiong, X.-H. Zhang, S.-F. Wang, *Biosens. Bioelectron.*, 99 (2018) 28–33.
67. K. Zhang, M. Pei, Y. Cheng, Z. Zhang, C. Niu, X. Liu, J. Liu, F. Guo, H. Huang, X. Lin, *J. Electroanal. Chem.*, 898 (2021) 115635.
68. Q.-L. Wang, H.-F. Cui, X. Song, S.-F. Fan, L.-L. Chen, M.-M. Li, Z.-Y. Li, *Sens. Actuators B Chem.*, 260 (2018) 48–54.
69. J. Zheng, J. Wang, D. Song, J. Xu, M. Zhang, *ACS Appl. Nano Mater.*, 3 (2020) 3449–3458.
70. C. Niu, X. Lin, X. Jiang, F. Guo, J. Liu, X. Liu, H. Huang, Y. Huang, *Bioelectrochemistry*, 143 (2022) 107986.
71. Z. Liu, S. Lei, L. Zou, G. Li, L. Xu, B. Ye, *Biosens. Bioelectron.*, 131 (2019) 113–118.
72. J. Li, L. Zhao, W. Wang, Y. Liu, H. Yang, J. Kong, F. Si, *Sens. Actuators B Chem.*, 328 (2021) 129031.
73. M. Mazloum- Ardakani, Z. Tavakolian- Ardakani, N. Sahraei, S.M. Moshtaghioun, *Biosens. Bioelectron.*, 129 (2019) 1–6.
74. Z. Liu, Y. Wang, Y. Guo, C. Dong, *Electroanalysis*, 28 (2016) 1023–1028.
75. D. Wang, Y. Li, Z. Lin, B. Qiu, L. Guo, *Anal. Chem.*, 87 (2015) 5966–5972.
76. Y.-L. Wang, J.-T. Cao, Y.-H. Chen, Y.-M. Liu, *Anal. Methods*, 8 (2016) 5242–5247.
77. X. Wei, X. Qiao, J. Fan, Y. Hao, Y. Zhang, Y. Zhou, M. Xu, *Microchem. J.*, 173 (2022) 106910.
78. G.-F. Shi, J.-T. Cao, J.-J. Zhang, K.-J. Huang, Y.-M. Liu, Y.-H. Chen, S.-W. Ren, *Analyst*, 139 (2014) 5827–5834.
79. Y. Zhao, L. Tan, G. Jie, *Sens. Actuators B Chem.*, 333 (2021) 129586.
80. B.-J. Shi, L. Shang, W. Zhang, L.-P. Jia, R.-N. Ma, Q.-W. Xue, H.-S. Wang, *Sens. Actuators B Chem.*, 344 (2021) 130291.
81. J.-J. Yang, J.-T. Cao, Y.-L. Wang, H. Wang, Y.-M. Liu, S.-H. Ma, *J. Electroanal. Chem.*, 787 (2017) 88–94.

82. F.-R. Liu, J.-T. Cao, Y.-L. Wang, X.-L. Fu, S.-W. Ren, Y.-M. Liu, *Sens. Actuators B Chem.*, 276 (2018) 173–179.
83. R. Han, Y. Sun, Y. Dai, D. Gao, X. Wang, C. Luo, *Sens. Actuators B Chem.*, 326 (2021) 128833.
84. L. Ge, W. Wang, T. Hou, F. Li, *Biosens. Bioelectron.*, 77 (2016) 220–226.
85. Z. Qiu, J. Shu, D. Tang, *Anal. Chem.*, 90 (2018) 12214–12220.
86. Z. Qiu, J. Shu, D. Tang, *Anal. Chem.*, 90 (2018) 1021–1028.
87. S. Lv, K. Zhang, L. Zhu, D. Tang, *Anal. Chem.*, 92 (2020) 1470–1476.
88. Z. Qiu, J. Shu, J. Liu, D. Tang, *Anal. Chem.*, 91 (2019) 1260–1268.
89. N. Zhou, X. Xu, X. Li, W. Yao, X. He, Y. Dong, D. Liu, X. Hu, Y. Lin, Z. Xie, D. Qu, C. Zhang, *Analyst*, 146 (2021) 5904–5912.
90. K. Zhang, S. Lv, Q. Zhou, D. Tang, *Sens. Actuators B Chem.*, 307 (2020) 127631.
91. X. Zeng, S. Ma, J. Bao, W. Tu, Z. Dai, *Anal. Chem.*, 85 (2013) 11720–11724.
92. S. Lv, K. Zhang, Q. Zhou, D. Tang, *Sens. Actuators B Chem.*, 310 (2020) 127874.
93. R. Yang, G. Jiang, J. Liu, Y. Wang, N. Jian, L. He, L. Liu, L. Qu, Y. Wu, *Anal. Chim. Acta*, 1153 (2021) 338283.
94. Z. Han, M. Luo, Q. Weng, L. Chen, J. Chen, C. Li, Y. Zhou, L. Wang, *Anal. Bioanal. Chem.*, 410 (2018) 6529–6538.
95. D. Huang, L. Wang, Y. Zhan, L. Zou, B. Ye, *Biosens. Bioelectron.*, 140 (2019) 111358.